Mg-related charge transitions in Mg-doped Ga2O3

Bhandari, Suman, Zvanut, M.

Suman Bhandari, M. E. Zvanut, "Mg-related charge transitions in Mg-doped Ga2O3," Proc. SPIE 11687, Oxide-based Materials and Devices XII, 116872A (5 March 2021); doi: 10.1117/12.2582040

SPIE.

Event: SPIE OPTO, 2021, Online Only

Mg-related charge transitions in Mg-doped Ga_2O_3

Suman Bhandari* and M E Zvanut,
Department of Physics, University of Alabama at Birmingham, 1300 University Blvd., Birmingham, Alabama 35233, USA

ABSTRACT

Gallium oxide (Ga_2O_3), an ultra-wide bandgap semiconductor with potential applications in power devices, may be doped with Mg to control the native n-type conductivity. The charge transitions associated with Mg in Mg-doped β-Ga_2O_3 crystals are studied using photoinduced electron paramagnetic resonance (photo-EPR) spectroscopy to understand the mechanisms that produce stable semi-insulating substrates. The steady state photo-EPR measurements are performed at 130 K by illuminating the samples with photon energy from 0.7 to 4.7 eV. Our results show that there are two transitions associated with Mg in the bandgap: onset of quenching of neutral Mg at 1.5 eV and excitation at 3.0 eV. The quenching threshold is consistent with several DFT predicted values for $Mg^{-/0}$ level. Therefore, we suggest the quenching is due to transition of an electron from the valence band to the neutral Mg. For photoexcitation, hole capture is the only viable process due to polaronic nature of neutral Mg in Ga_2O_3. The measurements demonstrate that electron excitation to impurities, such as Fe and Ir, does not contribute to creation of the holes. Further, gallium vacancies must not participate since their characteristic EPR spectrum is never seen. Thus, we speculate that the defects responsible for the hole formation and consequent excitation of the neutral Mg are oxygen vacancies.

Keywords: Gallium Oxide, EPR, photo-EPR, defects, defect level, optical absorption, charge transition

1. INTRODUCTION

Gallium oxide (β-Ga_2O_3) is an ultra-wide bandgap (4.6-4.9 eV) semiconductor, which has attracted considerable attention in recent years as the material has potential to offer better power device performances than currently used semiconductors such as SiC and GaN [1-3]. Moreover, large-scale native β-Ga_2O_3 substrates can be grown using cost effective melt methods that facilitate homoepitaxial growth of β-Ga_2O_3 device layers. The homoepitaxial growth can reduce lattice mismatch between the device layers and substantially lower the dislocation density in devices. However, the as-grown n-type conductivity must be controlled in order to produce reliable Ga_2O_3 devices [4]. While efficient n-type conductivity can be achieved by doping Ga_2O_3 with Sn, Si, or Ge, p-type doping is not likely to be produced using conventional growth methods [5, 6]. Nevertheless, based on the success in producing p-type material in GaN by Mg doping, several groups have grown Mg-doped Ga_2O_3 [7, 8]. The p-type doping of Ga_2O_3 was not realized due to self-localization of holes as predicted by the theoretical calculations and recent experimental studies [9-13]. Although p-type conductivity appears allusive, Mg doping does produce stable semi-insulating material that can be used in devices such as MESFETs [14, 15].

The defect level, a measure of the energy required to excite a carrier from a defect to band edges, must be evaluated to understand the efficacy of doping and mechanisms that enable production of stable semi-insulating substrates. Several hybrid functional calculations place the $Mg^{-/0}$ level between 1 eV and 1.6 eV above valence band maximum (VBM) [12, 13, 16, 17]. Consistently, photoinduced current transient spectroscopy suggest that a Mg-related hole trap lies 1.05 eV above VBM [18]. In contrast, by studying the thermal decay of neutral Mg (Mg^0) in Mg-doped Ga_2O_3 Lenyk et al suggest that the $Mg^{-/0}$ level is approximately 0.65 eV above VBM [19]. This latest experimental report of $Mg^{-/0}$ level questions the validity of the previously reported experimental and theoretical values. To help resolve the apparent discrepancies, we employ optical methods to probe transitions related to the Mg impurity. In addition to Mg, the method enables monitoring the presence of unintentionally added impurities such as Ir and Fe, which have defect levels ~2.6 eV above VBM and within 0.8 eV from band edges, respectively [4, 17, 20-22]. Other competing transitions may arise from intrinsic defects such as oxygen vacancies (V_O), gallium vacancies (V_{Ga}) and their complexes, which are predicted to be thermodynamically stable with defects levels that lie near mid gap [23, 24]. In order to understand charge transitions related to an intentional impurity such as Mg, the effect of all of these unintentional defects needs to be considered.

***email: omus1987@uab.edu**

Oxide-based Materials and Devices XII, edited by David J. Rogers, David C. Look
Ferechteh H. Teherani, Proc. of SPIE Vol. 11687, 116872A · © 2021 SPIE
CCC code: 0277-786X/21/$21 · doi: 10.1117/12.2582040

In the work discussed below, we report charge transitions related to Mg in Ga_2O_3 using photo-induced electron paramagnetic resonance (photo-EPR) spectroscopy. Photo-EPR involves the use of external photon energy that induces a change in EPR intensity. The change in EPR intensity reflects a transition of the defect from one charge state to the other. Thus, using photo-EPR, charge transitions between defects and the band edges may be investigated [25]. The present steady-state photo-EPR results show a photo-threshold for the quenching of Mg^0 as approximately 1.5 eV and for excitation as 3.0 eV, indicating that neutral Mg has two transition within the bandgap of Ga_2O_3.

2. EXPERIMENTAL DETAILS

Photo-EPR experiments were performed on two Mg-doped β-Ga_2O_3 crystals (S1 and S2) grown by the Czochralski method. Sample S1 was grown by Northrop Grumman Corporation, Synoptics, and sample S2 was grown by the Institute for Materials Research at Washington State University, Pullman, WA. Table I summarizes the concentrations of Mg, Fe, Cr, and Si determined by secondary ion mass spectrometry (SIMS). Since the Ir concentration determined by SIMS is uncalibrated due to a lack of a standard, we have no reliable measure of the total Ir concentration. However, the amount of Ir is estimated by determining the amount of Ir^{4+} detected by EPR as explained below.

An EPR signal was integrated twice numerically to obtain the integrated intensity, and was then compared with that of a calibrated Si:P powder to obtain the total amount of the EPR active center [26]. The calculated amount is accurate to no more than 50%. The average concentration throughout the sample was obtained by dividing by the volume of the sample. The concentration of Ir^{4+} ions (S = 1/2) detected using EPR in both samples is approximately 5×10^{17} cm^{-3}. Assuming the large concentration of Mg places the Fermi level below the $Ir^{3+/4+}$ level, we use this as the approximate amount of Ir.

Table I. The concentrations of impurities, 10^{17} cm^{-3}, in Mg-doped β-Ga_2O_3 samples measured by SIMS.

Impurity	Sample S1	Sample S2
[Mg]	25	33
[Fe]	0.7	0.06
[Cr]	0.1	0.03
[Si]	2.8	0.25

The dimensions (l x w x t) of the samples S1 and S2 were 5.0 mm x 2.8 mm x 1.3 mm and 7.6 mm x 2.8 mm x 0.7 mm, respectively. X-ray diffraction was performed to determine the crystal directions. For sample S1, the b-axis is the surface normal to the largest face (010), while the c-axis is nearly parallel to the length of the sample, and for sample S2, the largest face is (100) and the length is along the b-axis. Since an EPR signal represents a defect in a specific charge state, any change in the EPR amplitude represents a change in the charge state of the defect. In order to investigate charge transitions of impurities, photo-EPR experiments were performed at 9.4 GHz using light emitting diodes (LEDs). All measurements were carried out at 130 K with the magnetic field parallel to the a-axis. For photo-quenching experiments, first, a 280 nm LED (4.4 ± 0.2 eV) with 2 mW power was shone through the slits of the EPR cavity to generate the multiline spectrum typical of neutral Mg (Mg^0) in Mg-doped β-Ga_2O_3 [10]. Then, the samples were illuminated with LEDs of selected photon energy from 0.7-4.7 eV, using neutral density filters to maintain a constant photon flux. For steady state photo-EPR, a spectrum was obtained before and after the sample was illuminated with a specific photon energy for 25 min or until the EPR signal nearly saturated. Due to a slight decay of the signal after removing the light, the EPR 'after' spectra were measured at the end of the 25 min period while the sample remained illuminated. Before the next LED was used, the Mg^0 signal was completely quenched by raising the temperature to 260 K, waiting 2 min, returning to 130 K, and illuminating the sample with the 4.4 eV LED to regenerate the signal. After acquiring the steady state EPR signal for each photon energy, the relative change in the number of centers was calculated by comparing the EPR amplitudes before and after illumination. The total number of defects was determined as explained earlier using the signal with the largest amplitude

for sample S1. Then, by comparing the EPR amplitudes with the remaining spectra, including the sample S2, the number of centers for all other photon energies was calculated. The relative error in the relative concentrations is less than 10%. The concentrations of Mg^0 generated in samples S1 and S2 after illumination with the 4.4 eV LED for 25 min were 2 x 10^{17} cm^{-3} and 4 x10^{16} cm^{-3}, respectively. For photoexcitation, measurements were performed in the same manner as for photo-quenching, except that the 4.4 eV LED was not used before subsequent illumination with other LEDs.

3. RESULTS AND DISCUSSION

In Figure 1, we show EPR spectra of Mg^0 in sample S1 at 130 K with magnetic field along the a-axis. The center is EPR-silent in the dark (black); however, it can be changed to the EPR active state after the sample is illuminated with a 4.4 eV LED (blue). The red spectrum is an illustration of quenching of the 4.4 eV-generated signal during illumination with 2.5 eV. The spectrum, initially identified by Kananen et al, represents a hole on a non-bonding 2p orbital of an oxygen atom [10]. The decrease of the Mg^0 EPR intensity is quantified for selected photon energy in Figure 2a, where triangles represent sample S1 and circles, sample S2. Except for the first point, the vertical axis represents the difference in the concentration of Mg^0 before and after each photon energy. Once generated, the amount of neutral Mg decreases above 1.5 eV for both samples. The decrease indicates that Mg^0 becomes EPR silent during illumination. Here, we suggest that the decrease is due to excitation of an electron from the valence band to the defect, $Mg^0 + h\nu + e_V \rightarrow Mg^-$ (e_V is electron in the valence band). Above 3 eV, the amount of neutral Mg that is quenched begins to decrease, suggesting that a second, competing, process is initiated. Confirmation of the second process is seen in Figure 2b which shows the photoexcitation of Mg^0 from dark in samples S1 (triangles) and S2 (circles). For excitation, the change in the concentration is determined from the LED illumination with a constant flux of 1x10^{15} photons/s. The inset of Figure 2b displays the expanded view of the photoexcitation in sample S2. Both samples show that neutral Mg is generated during illumination with photon energy greater than 3 eV, the energy at which the amount of quenched neutral Mg (Fig. 2a) begins to decrease. Thus, it is clear that the change seen in Fig. 2a around 3 eV is due to the onset of a 2nd process. The fact that an order of magnitude less photon flux was sufficient to initiate the second process compared to quenching suggests that excitation of Mg^0 has a higher transition probability than quenching.

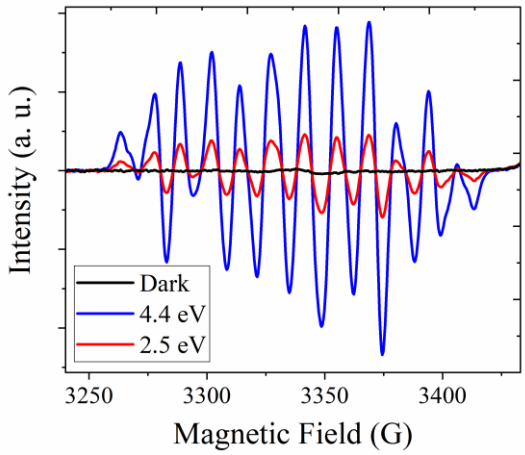

Figure 1. EPR spectra of neutral Mg in Mg-doped Ga_2O_3 before any illumination (black), and after subsequent illumination with 4.4 eV (blue) and 2.5 eV (red). The spectra were taken at 130 K with B //a.

3.1 Photo-quenching of Mg^0

Figure 3a shows the steady state photo-EPR for the quenching of Mg^0 in sample S1, along with the changes observed in Fe^{3+} (circles) and Ir^{4+} (stars). One can see a slight change in Fe^{3+} near the Mg^0 photo-threshold; however, that same threshold is present in purely Fe-doped samples. We also point out that the change is 1 to 2 orders of magnitude smaller than that seen for Mg^0, supporting the conclusion that Fe^{3+} could not be responsible for the Mg^0 transition. The Ir^{4+} changes are significant; however, as expected from the known mid-gap defect level, the threshold for the Ir^{4+} photoexcitation is well above the Mg^0 threshold. Thus, Ir^{4+} is also not involved in Mg^0 transition. Rather, we interpret the decrease in Mg^0 during photo-quenching as excitation of an electron from the valence band to the Mg^0 generated by the 4.4 eV light. We

note that the photo-quenching threshold of 1.5 eV is in stark contrast to the $Mg^{-/0}$ level, 0.65 eV above VBM, reported by Lenyk et al probing thermal decay of Mg^0 using EPR [19]. Surprisingly, we don't observe any change in the amount of Mg^0 for photon energy ≤1 eV during our 130 K measurements. Two observations support our identification of the optical transition as trapping of a valence band electron at Mg^0: 1. The quenching threshold is in reasonable agreement with the DFT calculated value for $Mg^{-/0}$, 1-1.6 eV above VBM [12, 13, 16, 17]. 2. The measurements require an order of magnitude larger photon flux than has been used in previous measurements, a fact likely related to the low transition probability expected between a p-like valence band electron and the hole orbital on the oxygen neighboring the Mg impurity.

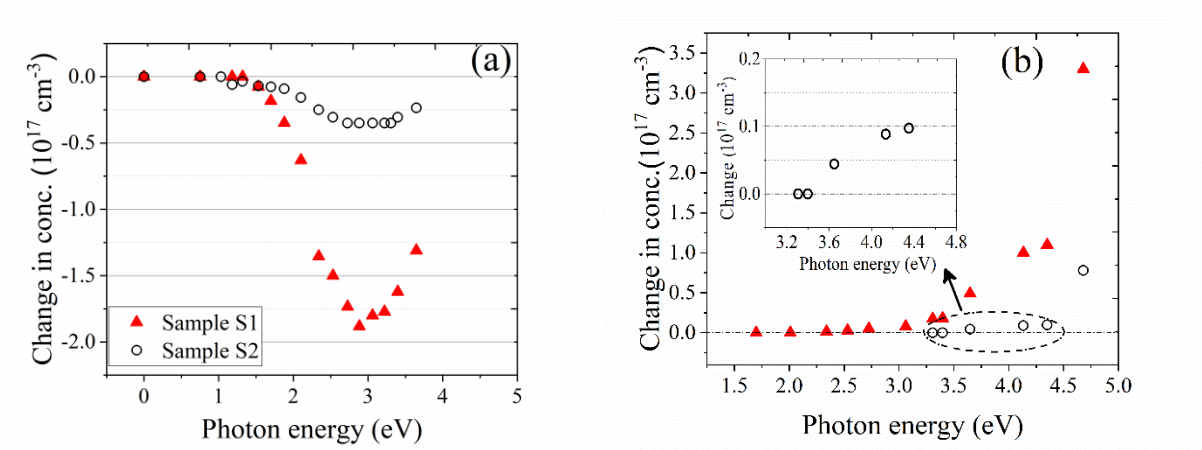

Figure 2. Steady state photo-EPR data for Mg^0 obtained on sample S1 (red triangles) and sample S2 (unfilled circles). (a) photo-quenching obtained with a flux of ~1×10^{16} photons/s, (b) photoexcitation using approximately 1×10^{15} photons/s. Inset: Expanded view of the photoexcitation data in sample S2.

Despite identification of the 1.5 eV photo-EPR threshold as an optically induced valence band-to-Mg^0 transition, the assignment of the $Mg^{-/0}$ level remains unclear. In our previous work, we showed that accurate determination of a defect level by optical techniques requires consideration of the structural relaxation of the lattice around the defect as it changes charge state. In reference 22, we determined the transition level for $Fe^{2+/3+}$ in Ga_2O_3 by incorporating lattice relaxation into analysis of the optical cross section spectrum that had been obtained from the time-dependent photo-EPR data for Fe^{3+} [22]. Whether, in the case of Mg^0, the predicted 1 eV relaxation energy is sufficient to account for the difference between the experimentally predicted defect level of 0.65 eV and the 1.5 eV photo-threshold observed here awaits thorough analysis of the time-dependent EPR data [27].

3.2 Photoexcitation of Mg^0

When a defect such as Mg^0 captures electrons from the valence band via $Mg^0 + e_V \rightarrow Mg^-$, reverse process, $Mg^- + h\nu \rightarrow Mg^0 + e_C$, might also be expected to occur (e_C is electron in the conduction band). This is particularly true for a semiconductor like Ga_2O_3 where the ultrawide bandgap provides an energy range sufficient to encompass both processes. Indeed, as shown in Figure 2b, Mg^0 reappears at photon energy of about 3 eV. The threshold for quenching, 1.5 eV, and this threshold for excitation, 3 eV, sum to approximately the bandgap, consistent with identification of the latter threshold with excitation of an electron from the defect to the conduction band. However, both theory and experiment confirm that the neutral Mg represented by the EPR signal is a hole trapped on a near neighbor oxygen atom and forms a polaronic state [10, 12, 13]. As such, once an electron is trapped at this defect, a deep gap state no longer exists [12]. Thus, given the accepted model for Mg^0, the reverse process, $Mg^- + h\nu \rightarrow Mg^0 + e_C$, may not be considered. Rather, the quenching of Mg^0 must occur by hole capture from the valence band. Below we discuss possible mechanisms for the hole capture.

Figure 3b shows that hole formation in the valence band cannot occur due to excitation of either of the dominant impurities, Fe or Ir. Here, the triangles represent Mg^0, circles Fe^{3+}, and stars Ir^{4+} in sample S1. Similar results are observed in sample S2. One can see that the Fe^{3+} change is minimal and Ir^{4+} changes erratically. While data show that neither are major sources

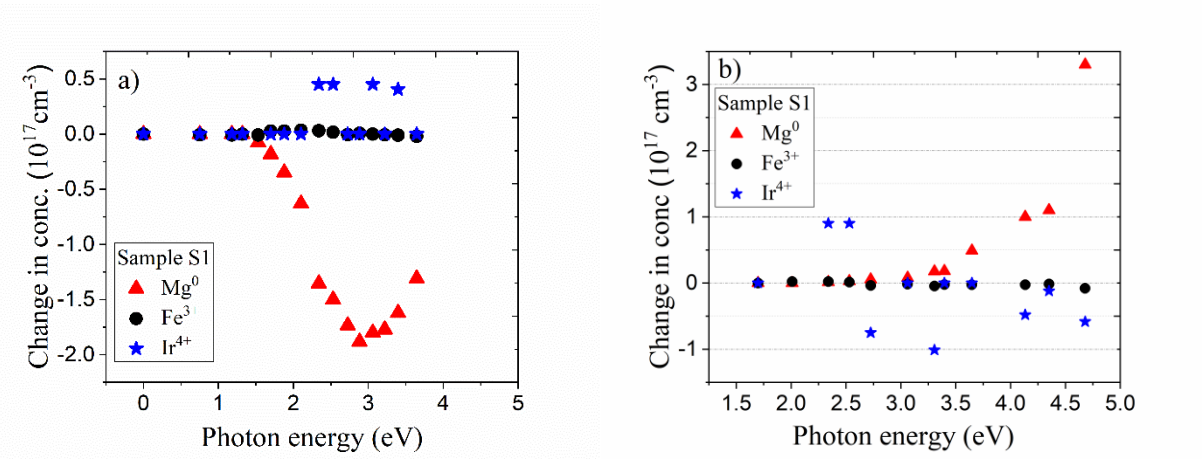

Figure 3. Steady state photo-EPR data for neutral Mg (triangles), Ir^{4+} (stars), and Fe^{3+} (circles) obtained on sample S1. (a) photo-quenching was obtained with a flux of ~1 × 10^{16} photons/s; (b) photoexcitation using approximately 1 × 10^{15} photons/s.

of hole creation, the defect responsible for the holes is not clear. Of the simplest intrinsic defects, V_O and V_{Ga}, several charge states of the latter are EPR-active but not seen during our measurements despite observations by others [28-30]. Thus, we eliminate them from consideration. Both stable charge states of V_O are EPR inactive, so we can only speculate as to their role in the excitation process for Mg^0. Based on the observation of both Fe^{3+} and Ir^{4+} before illumination, together with the accepted $Ir^{3+/4+}$ defect level of 2.6 eV above VBM, we conclude that that the Fermi level is initially in the lower half of the bandgap. The defect levels for V_O, $V_O^{0/2+}$, range from 2 eV to 3.5 eV above VBM [23, 31], so some of the vacancies are in the 2+ charge state. During illumination, then, electrons can transition to V_O^{2+}, generating holes in the valence band and hence Mg^0. The partial s-character of V_O supports the likelihood of electron transfer from the p-like valence band and is consistent with the order of magnitude less photon flux needed to observe excitation compared to quenching. Furthermore, the negative U character, makes V_O an efficient center for hole creation.

In summary, photoinduced EPR has identified two transitions for the substitutional Mg impurity in Ga_2O_3. The neutral Mg EPR signal created by 4.4 eV light may be quenched with energy as low as 1.5 eV and then re-excited at approximately 3 eV. The 1.5 eV photo-threshold for quenching is remarkably larger than $Mg^{-/0}$ level reported experimentally by others; however, the threshold is in reasonable agreement with DFT transition calculated by several groups [12, 13, 16, 17, 19]. The model for Mg^0 dictates that the re-excitation at energy greater than 3 eV must occur by hole capture from the valence band, but the mechanism responsible for creation of the hole is not clear. Neither of the common impurities, Fe or Ir, correlate with the Mg^0 excitation and V_{Ga} is never observed; thus, we speculate that the hole is generated by capture of a valence band electron at an oxygen vacancy.

ACKNOWLEDGEMENTS

The work is supported by the National Science Foundation (NSF) Grant: DMR-1904325. We acknowledge Luke Sande, NG Synoptics, and Jani Jesenovec and Matthew D. McCluskey, Washington State University for providing the Mg-doped Ga_2O_3 samples. We also appreciate useful conversations with John Lyons and Darshana Wickramaratne at US Naval Research Laboratory.

REFERENCES

[1] Ueda, N., Hosono, H., Waseda, R., and Kawazoe, H., "Anisotropy of electrical and optical properties in β-Ga_2O_3 single crystals", App. Phys. Lett. **71**(7), 933 (1997).

[2] Pearton, S. J., Yang, J., Cary, P. H., Ren, F., Kim, J., Tadjer, M. J., and Mastro, M. A., "A review of Ga_2O_3 materials, processing, and devices", Appl. Phys. Rev. **5**(1), 011301 (2018).

[3] Higashiwaki, M., Sasaki, K., Kuramata, A., Masui, T., and Yamakoshi, S., "Development of gallium oxide power devices", Phys. Status Solidi A **211**(1), 21–26 (2014).

[4] Kuramata, A., Koshi, K., Watanabe, S., Yamaoka, Y., Masui, T., and Yamakoshi, S., "High-quality β-Ga_2O_3 single crystals grown by edge-defined film-fed growth", Jpn. J. Appl. Phys. **55**(12), 1202A2 (2016).

[5] Baldini, M., Albrecht, M., Fiedler, A., Irmscher, K., Schewski, R., and Wagner, G., "Si- and Sn-Doped Homoepitaxial β-Ga_2O_3 Layers Grown by MOVPE on (010)-Oriented Substrates", ECS J Solid State Sci and Technol., **6**(2), Q3040-Q3044 (2017).

[6] Han, S. H., Mauze, A., Ahmadi, E., Mates, T., Oshima, Y., and Speck, J. S., "n-type dopants in (001) β- Ga_2O_3 grown on (001) β-Ga_2O_3 substrates by plasma-assisted molecular beam epitaxy", Semicond. Sci. Technol. **33**(4), 045001 (2018).

[7] Nakamura, S., Senoh, M., Mukai, T., "Highly P-Typed Mg-Doped GaN Films Grown with GaN Buffer Layers", Jpn. J. Appl. Phys. **30**(10A), L1708-L1711 (1991).

[8] Nakamura, S., Mukai, T., Senoh, M., and Iwasa, N., "Thermal Annealing Effects on P-type Mg-doped GaN Films", Jpn. J. Appl. Phys. **31**(2B), part 2, L139-L142 (1992).

[9] Kananen, B. E., Giles, N. C., Halliburton, L. E., Foundos, G. K., Chang, K. B., Stevens, K. T., "Self-trapped holes in β-Ga_2O_3 crystals", J. Appl. Phys. **122**(21), 215703 (2017).

[10] Kananen, B. E., Halliburton, L.E., Scherrer, E. M., Stevens, K. T., Foundos, G. K., Chang, K. B., and Giles, N. C., "Electron paramagnetic resonance study of neutral Mg acceptors in β-Ga_2O_3 crystals", Appl. Phys. Lett. **111**(7), 072102 (2017).

[11] Varley, J. B., Janotti, A., Franchini, C., and Van de Walle, C. G., "Role of self-trapping in luminescence and p-type conductivity of wide-band-gap oxides", Phy. Rev. B **85**(8), 081109(R) (2012).

[12] Lyons, J. L., "A survey of acceptor dopants for β-Ga_2O_3", Semicond. Sci. Technol. **33**(5), 05LT02 (2018).

[13] Ho, Q. D., Frauenheim, T., and Deak, P., "Theoretical confirmation of the polaron model for the Mg acceptor in β-Ga_2O_3", J. Appl. Phys. **124**(14)**,** 145702 (2018).

[14] Onuma, T., Fujioka, S., Yamaguchi, T., Higashiwaki, M., Sasaki, K., Masui, T., and Honda, T., "Correlation between blue luminescence intensity and resistivity in β-Ga_2O_3 single crystals", Appl. Phys. Lett. **103**(4), 041910 (2013).

[15] Higashiwaki, M., Sasaki, K., Kuramata, A., Masui, T., and Yamakoshi, S., "Gallium oxide (Ga_2O_3) metal-semiconductor field-effect transistors on single-crystal β-Ga_2O_3 (010) substrates", Appl. Phys. Lett. **100**(1), 013504 (2012).

[16] Kyrtsos, A., Matsubara, M., and Bellotti, E., "On the feasibility of p-type Ga_2O_3", Appl. Phys. Lett. **112**(3), 032108 (2018).

[17] Ritter, J. R., Huso, J., Dickens, P. T., Varley, J. B., Lynn, K. G., and McCluskey, M. D., "Compensation and hydrogen passivation of magnesium acceptors in β-Ga_2O_3", Appl. Phys. Lett. **113**(5), 052101 (2018).

[18] Polyakov, A. Y., Smirnov, N. B., Shchemerov, I. V., Yakimov, E. B., Pearton, S. J., Ren, F., Chernykh, A. V., Gogova, D., and Kochkova, A. I., "Electrical Properties, Deep Trap and Luminescence Spectra in Semi-Insulating, Czochralski β-Ga_2O_3(Mg)", ECS J Solid State Sci and Technol., **8**(7), Q3019-Q3023 (2019).

[19] Lenyk, C. A., Gustafson, T. D., Basun, S. A., Halliburton, L. E., and Giles, N. C., "Experimental determination of the (0/-) level for Mg acceptors in β-Ga_2O_3 crystals", Appl. Phys. Lett. **116**(14), 142101 (2020).

[20] Ingebrigtsen, M. E., Varley, J. B., Kuznetsov, A. Y., Svensson, B. G., Alfieri, G., Mihaila, A., Badst bner, U., and Vines, L., "Iron and intrinsic deep level states in Ga_2O_3", Appl. Phys. Lett. **112**(4), 042104 (2018).

[21] Bhandari, S., and Zvanut, M. E., "Optical transitions for impurities in Ga_2O_3 as determined by photo-induced electron paramagnetic resonance spectroscopy", J. Appl. Phys. **127**(6), 065704 (2020).

[22] Bhandari, S., Zvanut, M. E., and Varley, J. B., "Optical absorption of Fe in doped Ga_2O_3", J. Appl. Phys. **126**(16), 165703 (2019).

[23] Deak, P., Ho, Q. D., Seemann, F., Aradi, B., Lorke, M., and Frauenheim, T., "Choosing the correct hybrid for defect calculations: A case study on intrinsic carrier trapping in β-Ga_2O_3", Phy. Rev. B **95**(7), 075208 (2017).

[24] Varley, J. B., Peelaers, H., Janotti, A., and Van deWalle, C. G., "Hydrogenated cation vacancies in semiconducting oxides", J. Phys.: Condens. Matter **23**(33)**,** 334212 (2011).

[25] Godlewski, M., "On the application of the photo-EPR technique to the studies of photoionization, DAP recombination, and non-radiative recombination processes", Phys. Status Solidi A **90**(1), 11 (1985).

[26] Weil, J., and Bolton, J., [Electron Paramagnetic Resonance: Elementary Theory and Practical Applications], John Wiley & Sons, Inc., pp. 545–546 (2007).

[27] Lyons, J. L., and Wickramaratne, D., Private Communication, 2021.

[28] Kananen, B. E., Halliburton, L. E., Stevens, K. T., Foundos, G. K., and Giles, N. C., "Gallium vacancies in β-Ga_2O_3 crystals", Appl. Phys. Lett. **110**(20), 202104 (2017).

[29] Son, N. T., Ho, Q. D., Goto, K., Abe, H., Ohshima, T., Monemar, B., Kumagai, Y., Frauenheim, K., and Deak, P., "Electron paramagnetic resonance and theoretical study of gallium vacancy in β-Ga_2O_3", Appl. Phys. Lett. **117**(3), 032101 (2020).

[30] Skachkov, D., Lambrecht, W. R. L., von Bardeleben, H. J., Gerstmann, U., Ho, Q. D., and Deak, P., "Computational identification of Ga-vacancy related electron paramagnetic resonance centers in β-Ga_2O_3", J. Appl. Phys. **125**(18), 185701 (2019).

[31] Varley, J. B., Weber, J. R., Janotti, A., and Van de Walle, C. G., "Oxygen vacancies and donor impurities in β-Ga_2O_3", Appl. Phys. Lett. **97**(14), 142106 (2010).